Neutral Gas Puffing Effects on the Density Pedestal in High-Confinement DIII-D Plasmas

A thesis submitted in partial fulfillment of the requirement
for the degree of Bachelor of Science in
Physics from the College of William and Mary in Virginia,

by

Peter Kress

Advisor: Prof. Saskia Mordijck

Williamsburg, Virginia
May 2018

Contents

Acknowledgments **iii**

List of Figures **vii**

List of Tables **viii**

Abstract **v**

1 Introduction **1**

1.1 Fusion 1

1.2 Tokamaks 2

1.3 The Pedestal 4

2 Theory **6**

2.1 Theory Introduction 6

2.2 Fueling and Penetration Depth 6

2.3 Divertor Geometry 7

2.4 Fueling Theory 7

3 Experimental Analysis **11**

3.1 Introduction 11

3.2 Preparation 13

3.3 Analysis and Results 14
3.3.1 Analytical Method 14
3.3.2 Aggregate Results 14
3.3.3 In Depth Results 16
3.3.4 Analysis of Results 18

4 Conclusions and Future Plans **27**

4.1 Conclusions 27
4.2 Future Study 29

Acknowledgments

Many thanks to Professor Mordijck, Professor Mikhailov, and Professor Novikova. Your mentorship has meant the world to me and genuinely changed my life.

Additional thanks to friends and family for constant support and encouragement.

List of Figures

1.1 An illustration of a deuterium-tritium fusion reaction. When a deuterium ion collides with a tritium ion, the nuclear strong force combines them into a single helium nucleus releasing a neutron and energy as byproducts[1]. 2

1.3 A tokamak confines plasma with magnetic fields by creating strong toroidal and poloidal magnetic fields that propel plasma around the torus while containing it to a D-shape with minimal connection to the vessel surface[3]. 3

1.2 Cross section of a tokamak plasma. 4

1.4 Plots illustrating temperature, density, and pressure pedestals within the edge of tokamak plasmas vs Ψ[2]. 5

2.1 Gas flows more freely within open divertor plasmas than closed divertor plasmas because of more space for the neutral gas to diffuse. The cryo-pump is located at the top of the tokamak, causing it to more efficiently remove neutrals in closed divertor plasmas. 8

2.2 Density profile and fueling vs normalized magneto-radius. Density profiles observed in the core are caused by transport because there are no fueling effects. It is more complicated to discern transport effects at the edge where fueling is present. 10

3.1 Thomson Scattering diagnostic measurement points (red) overlayed onto a plasma cross section. To compare the Thomson Scattering data we need to change coordinate systems to control for magnetic and radial differences in the plasma. 20
3.2 Filterscope diagnostic measurement points (blue and green) overlayed onto a plasma cross section. The filterscope diagnostic that experiences the least noise in its signal is the diagnostic closes to the strike point, which in this case is FS01. 20
3.3 ELM cycles over time in a relatively predictable plasma with consistent ELM patterns. Using a critical filter value works well for this data. . 21
3.4 ELM cycles over time in a relatively messy plasma with inconsistent ELM patterns. Using a critical filter value ignores the dynamics of the plasma, making it a suboptimal filtering technique. 21
3.5 Time response of plasma through an ELM cycle. After about 10ms the density values are stable at their equilibrium levels again. This figure shows the density across the pedestal from just inside the edge at $\rho = 0.96$ to just outside at $\rho = 1.02$. We see a drop in density inside that recovers back to normal levels, while we see a peak in density outside that recovers back to normal levels [4]. 21
3.6 Data dispersion and tanh fit for a HighIp plasma without filtering ELM patterns. 22
3.7 Data dispersion and tanh fit for a HighIp plasma with ELM filtering. The spread of the data with filtering is substantially lower than without filtering, making the fits more dependable. 22
3.8 Tanh fit for a filtered HighIp plasma with consistent ELMs 22
3.9 Tanh fit for a filtered closed divertor plasma with inconsistent ELMs. 22

3.10 Ne_{SOL} and Ne_{Ped} vs fueling for each plasma type Find very similar relationships for the scrape off layer, but more diverse relationships for the pedestal top. 22
3.11 The difference in density across the pedestal vs fueling for all plasma types. The difference in density gives insight into how fueling increases density at the pedestal top and scrape off layer at the same time. We see than in terms of scale, the top of the pedestal increases by more than the base. 23
3.12 The pedestal fit parameters for height and width vs fueling. Pedestal relative height is consistently downward sloping across all plasma types, but pedestal width responses are not as consistent. Both open divertor pedestal widths exhibit negative correlations, but the open divertor plasma width exhibits a postive correlation to fueling. 23
3.13 Density at the scrape off layer vs fueling separated by plasma type. Only the open divertor plasmas have significant correlations with fueling. The correlations were very similar despite varied plasma conditions. 24
3.14 Density at the pedestal vs fueling separated by plasma type. Only the open divertor plasmas have significant correlations with fueling. Found more disparate correlations with fueling than the scrape off layer density. 24
3.15 Density difference across the pedestal vs fueling separated by plasma type. Only the open divertor plasmas have significant correlations with fueling. The lower density Open plasmas has more significant growth across the pedestal than HighIp plasmas. 25
3.16 Normalized pedestal height parameter vs fueling separated by plasma type. Only the high current plasmas have significant correlations with fueling. 25

3.17 Pedestal width parameter vs fueling separated by plasma type. None of the plasma types had significant correlations with fueling. 26

List of Tables

3.1 Regression statistics for scrape off layer density vs fueling. 16
3.2 Regression statistics for pedestal density vs fueling. 17
3.3 Regression statistics for the change in density across the pedestal vs fueling. 17
3.4 Regression statistics for the height parameter across the pedestal vs fueling. 18
3.5 Regression statistics for the width parameter across the pedestal vs fueling. 18

Abstract

Particle transport effects at the edge of tokamak plasmas are important for designing feasible fusion reactors. Understanding particle transport plasmas requires isolating the effects on plasma density. This project investigates density responses to neutral fueling across the pedestal to determine the role of fueling in density profile formation. We investigated density profile responses to various neutral fueling levels by analyzing plasmas from the DIII-D fusion research facility. For open divertor plasmas, fueling increases density in the plasma edge, with stronger effects at the scrape off layer than the pedestal top. However, fueling has no substantial effect on the pedestal width, though for higher density plasmas this may not be the case. We found substantial differences between open and closed divertor plasma responses to fueling.

Chapter 1

Introduction

1.1 Fusion

Nuclear fusion, the process by which the sun heats the solar system, releases energy proportional to the reduction in mass when two atoms fuse together, given by Einstein's famous equation $E = mc^2$. The amount of energy released through fusion is enormous relative to the amount of fuel required. Harnessing fusion energy could solve many environmental and economic problems surrounding energy production.

Atomic nuclei will fuse into a single larger nucleus if they get close enough for the nuclear strong force to bring them together. Because, the nuclear strong force only acts over short distances, nuclei must first overcome the electromagnetic repulsion they experience as like charges, called the Coulomb barrier. In stars, gravitational forces drive nuclei to fuse. The consequential release of energy facilitates further fusion as nearby nuclei are energized. This chain reaction continues until all nuclei have fused into heavy elements and no longer release energy by fusing. Gravitational forces partially ionize gases in stars, creating plasmas which are necessary for fusion to occur. In a plasma, nuclei become separated from their orbiting electrons. The electrons and ions still interact, maintaining a quasi-neutral equilibrium. However, ions are not longer shielded from other ions by electron shells which ordinarily prevent

nuclear collisions. Because the charged particles are free to move in a plasma, plasmas are not only affected by collisions but also by magnetic fields according to the Lorentz force $\mathbf{F} = q\mathbf{v} \times \mathbf{V}$. Plasma can therefore be modeled as a magnetically sensitive fluid.

For deuterium ions to be energetic enough to overcome the Coulomb barrier, a plasma needs to be extremely high energy. Furthermore, the super-heated plasmas must be contained in such a way to prevent cooling, instability, and damage to device materials. Necessary conditions for consistent fueling, called burning plasma conditions, have not yet been achieved simultaneously. However, each necessary condition, e.g. temperature, density, pressure, stability, etc., has been achieved independently.

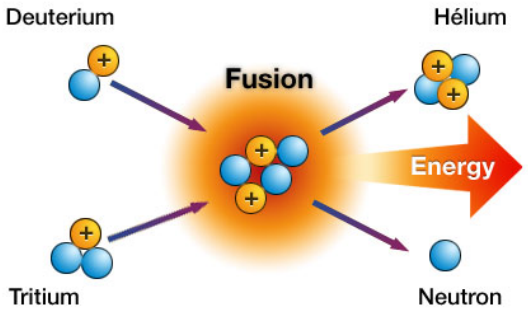

Figure 1.1: An illustration of a deuterium-tritium fusion reaction. When a deuterium ion collides with a tritium ion, the nuclear strong force combines them into a single helium nucleus releasing a neutron and energy as byproducts[1].

1.2 Tokamaks

This paper uses data from the DIII-D Fusion Research Facility tokamak. The tokamak, shown in figure 1.3, is a promising plasma confinement design which use strong magnetic fields to guide plasma along a torus. This torus is made up of many identical electromagnets that create strong toroidal magnetic fields to contain the plasma. Because of the symmetry of the tokamak, plasma cross sections, shown in figure 1.2, are essentially identical at any point along the torus. To propel the plasma around the tokamak, poloidal magnetic fields are pulsed to induce plasma current. This current induces poloidal magnetic fields which further confine the plamsa. With

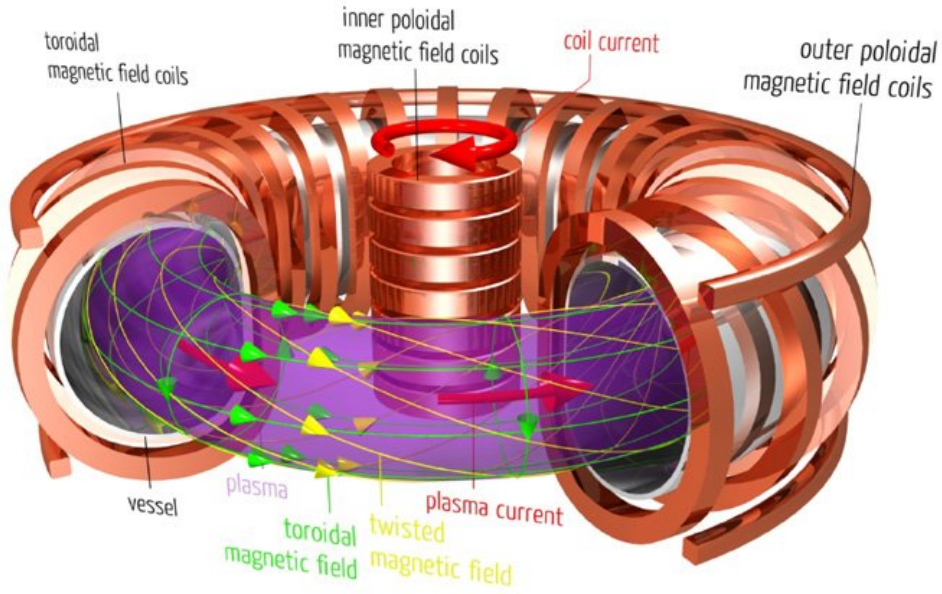

Figure 1.3: A tokamak confines plasma with magnetic fields by creating strong toroidal and poloidal magnetic fields that propel plasma around the torus while containing it to a D-shape with minimal connection to the vessel surface[3].

sufficient field strength and plasma current, Lorentz forces stabilize the plasma and provide effective confinement.

Because tokamaks use magnetic fields to confine plasma, a plasma's magnetic environment must be considered in addition to its spatial environment. Concentric magnetic field lines build up the magnetic field from the edge to the core, creating magnetic flux surfaces around the torus. The magnetic fields propel plasma around the torus while containing it to a D-shape with minimal interaction with the tokamak wall. Plasmas occupy varying spaces in time as well as between experiments, leading to inconsistent spatial locations for their magnetic fields. However, the plasma diagnostics are fixed in space. To address this, we must include magnetic field information within the coordinate system of our analysis. We changed coordinates to a magneto-radial system, normalized flux Ψ_n, which ranges from 0 at the core to 1 at the final closed field line of the plasma. This is important because it allows for

comparison between diagnostics across the plasma and between experiments despite variation in the spatial and magnetic parameters.

Fusion requires enormous pressure within a plasma. As a result, maximizing the confinement capabilities of tokamaks can significantly improve plasma conditions. Steep increases in temperature and density, called pedestals, occur in the edge region of a tokamak plasma.

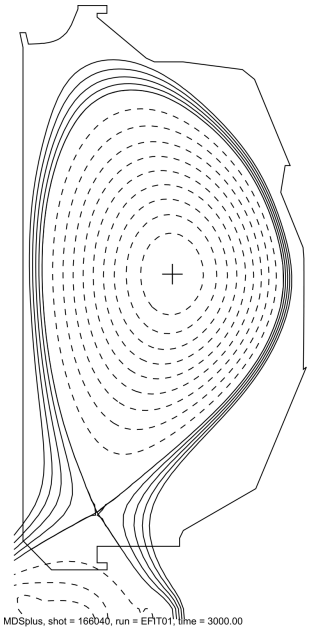

Figure 1.2: Cross section of a tokamak plasma.

1.3 The Pedestal

Optimizing plasma performance in a tokamak is constrained by ensuring the tokamak itself remains undamaged. Tokamak walls and diagnostics are unable to endure direct exposure to fusing plasma. To protect the machine, the plasma must be relatively cold at its edge. However, the relatively cold plasma does not fuse quickly enough for energy production. To optimize the amount of volume with efficient fusion, plasmas require steep density and temperature gradients at their edge. This allows the tokamak materials to remain safe while providing a relatively large volume for fusion conditions.

The pressure differential between the core and the edge causes plasma at the core to leak out toward the low pressure chamber. In order to combat this leakage, deuterium fuel is pumped into the chamber through neutral gas puffing. The neutral gas diffuses through the chamber, eventually colliding with the plasma. As it collides

with the plasma, the gas ionizes and joins the plasma. However, the gas is unaffected by magnetic fields until it is ionized, allowing it to bypass magnetic transport barriers. The gas ionizes as it penetrates into the plasma, increasing the plasma density where it ionizes.

This thesis will give prerequisite theory relevant to analyze and interpret neutral gas puff fueling in plasmas. It will then describe the process, assumptions, and results of our experimental analysis. Lastly, it will outline important future work for understanding edge transport effects with this analysis.

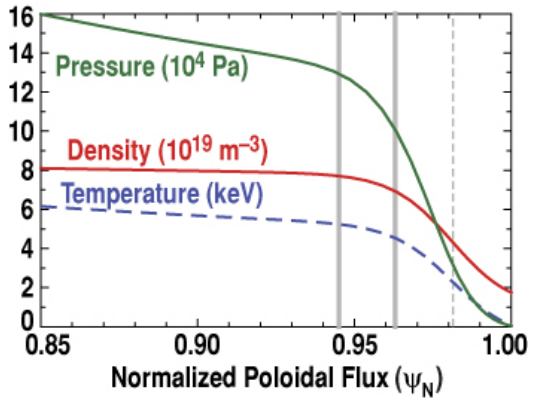

Figure 1.4: Plots illustrating temperature, density, and pressure pedestals within the edge of tokamak plasmas vs Ψ[2].

Chapter 2

Theory

2.1 Theory Introduction

It is important for the long term viability of tokamak designs in fusion energy research to understand transport effects at the edge of tokamak plasmas. In order to understand transport effects, fueling must be understood as well. This section demonstrates how the investigation of fueling effects contributes to understanding transport effects at the edge and summarizes the theory relevant to this analysis.

2.2 Fueling and Penetration Depth

Neutral gas fueling is important in tokamak plasmas because it provides additional fuel to the fusing plasma in addition to increasing external pressure to combat the loss of fuel from leakage. Deuterium enters the tokamak chamber in two ways. The first is through recycling: ionized deuterium exits the plasma through fuel leakage and recombines with electrons at the wall. The second is through the injection of deuterium gas from outside the tokamak into the tokamak chamber.

As the deuterium in the chamber diffuses, it eventually collides with the plasma and ionizes. When deuterium is neutral, electromagnetic fields do not influence its trajectory. As a result, neutrals can bypass electromagnetic transport barriers and

provide additional fuel to the interior of the plasma. However, the deuterium will ionize as it collides with the high energy plasma. The rate at which it ionizes is dependent on its interactions with the plasma around it. Since entering a dense plasma will lead to more collisions, higher density plasma increases the ionization rate of penetrating neutrals. The increase in density across the pedestal suggests that deuterium will penetrate the furthest edge of a plasma, called the scrape off layer, with relative ease, but ionize more quickly upon crossing the pedestal. As a result, deuterium that diffuses into the plasma is unlikely to make it into the core.

2.3 Divertor Geometry

Tokamaks can have open or closed divertor configurations. An open divertor allows for more deuterium to enter the chamber through recycling. A closed divertor, however, limits the ability of recycled deuterium to reenter the chamber by capturing it in the divertor area. At DIII-D, the plasma-wall interaction occurs closer to the cryo-pump for closed divertor configurations. The cryo-pump filters neutrals out of the chamber, so the closed divertor plasma is much more efficient at removing neutrals from the plasma. As a result, we expect neutral gas fueling to be less effective for closed divertor plasmas than open divertor plasmas. Figure 2.1 shows cross sections for closed and open divertor plasmas.

2.4 Fueling Theory

Because mass must be conserved in a volume over time, plasma density is described by the differential continuity equation

$$\frac{dn}{dt} = -\nabla\Gamma + S \tag{2.1}$$

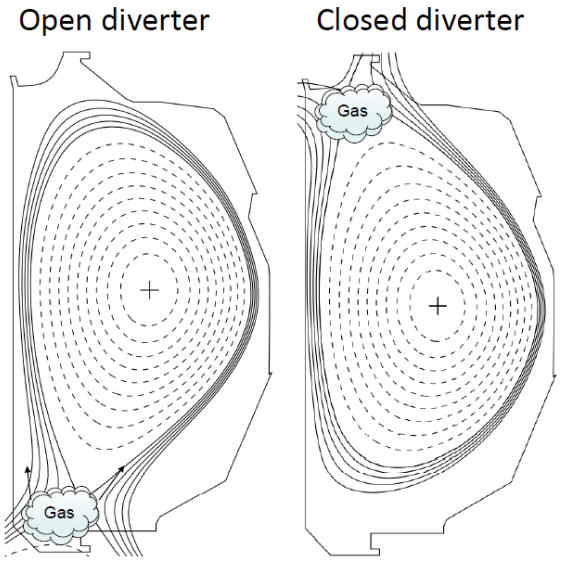

Figure 2.1: Gas flows more freely within open divertor plasmas than closed divertor plasmas because of more space for the neutral gas to diffuse. The cryo-pump is located at the top of the tokamak, causing it to more efficiently remove neutrals in closed divertor plasmas.

where $\frac{dn}{dt}$ is the change in density over time, Γ is the particle flux, and S is an external source term. When a plasma is stable, there is no change in density over short timescales at any point in the plasma on average, so $\frac{dn}{dt} = 0$. The continuity equation can then be rewritten as

$$\nabla\Gamma = S \tag{2.2}$$

For tokamak plasmas, the flux contains the transport effects and the source contains fueling effects. Flux is the combination of diffusion and convection effects described by the equation

$$\Gamma = -D\nabla n + Vn \tag{2.3}$$

where n is the density, D is the diffusion coefficient, and V is the flow velocity. Equation 2.3 can be rewritten to reflect the density gradient for the plasma

$$\frac{\nabla n}{n} = \frac{V}{D} - \frac{\Gamma}{Dn} \tag{2.4}$$

or to reflect the relative effects of diffusion and convection

$$\frac{V}{D} = \frac{\nabla n}{n} + \frac{\Gamma}{Dn} \tag{2.5}$$

At the core, there is no source term because fueling is not present because neutrals ionize as they penetrate the plasma. This implies $\nabla\Gamma = 0$ from equation 2.2, i.e. flux is constant in space and transport is constant in the plasma. If transport is constant, the density gradient would give direct insight into the relative effects of diffusion and convection, $\frac{V}{D}$, through equation 2.5 because the flux term would be constant. While approximating transport as constant in space might be valid at the core of a tokamak, it is not valid at the edge where fueling is present. Source and density profiles are shown in figure 2.2.

Flux can be related to the source term by integrating the continuity equation in a stable plasma, yielding $\Gamma = \int SdV$. Substituting this term into equation 2.5 we find

$$\frac{V}{D} = \frac{\nabla n}{n} + \frac{\int SdV}{Dn} \tag{2.6}$$

This analysis seeks to find preliminary information on the fueling term $\frac{\int SdV}{Dn}$ of equation 2.6 by investigating fueling effects on density at the edge.

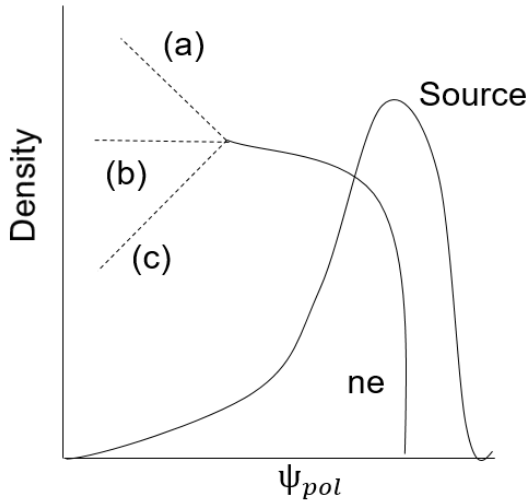

Figure 2.2: Density profile and fueling vs normalized magneto-radius. Density profiles observed in the core are caused by transport because there are no fueling effects. It is more complicated to discern transport effects at the edge where fueling is present.

Chapter 3

Experimental Analysis

3.1 Introduction

We selected plasma discharges with neutral gas fueling from 0 Torr×L/s to 300 Torr×L/s to compare neutral fueling effects on density across the pedestal region. I used 5 low current plasmas with an open divertor (Open), 5 low current plasmas with a closed divertor (Closed), and 10 high current plasmas with an open divertor (HighIp). These discharges were planned specifically to investigate plasma edge dynamics over time with different neutral gas fueling levels. The magnitude of the plasma current is directly linked to the strength of the poloidal magnetic fields, improving confinement. As a result, higher plasma current leads to higher plasma density. We identified a 500 ms window of time where shot parameters are relatively stable for each discharge.

We used density and temperature data from the Thomson Scattering diagnostic, shown in figure 3.1, for the discharges over the selected time windows. We changed the coordinates so the distance is normalized along the magnetic field lines, not spatial distance. This allows for the comparison of the Thomson Scattering data despite the non-uniform plasma shapes across experiments.

These plasmas undergo periodic structural fluctuations from edge localized modes (ELMs). ELMs are instabilities that result in the release of pressure from within the

plasma out through the edge. The spikes in figures 3.3 and 3.4 illustrate the release of plasma, captured by diagnostic measurements in the divertor region. This build up of density, shown in figure 3.5, saturates as it approaches the next release. As a result of the saturation, the plasma is relatively stable in the moments before an ELM. In order to avoid density changes that result from ELMs, we analyzed data from diagnostics that record ELM information, called filterscopes, and only used Thomson Scattering data from the last 20% of an ELM cycle.

Even within the more noisy plasma data, there are clear troughs in which the filterscope data is stable as it approaches an ELM. However, it can be difficult to identify the beginnings and ends of the ELM cycles because ELMs do not always have the same profile nor do they occur at a constant frequency. To account for these problems, we inspected each filterscope plot which shows the ELM releases over time to identify a reasonable height cutoff to qualify a peak as an ELM instead of noise or another type of instability. Even with visual inspection it is difficult to properly identify ELMs because the plasma can drift over time or undergo small fluctuations between ELMs, making a simple height cutoff an imprecise tool.

Not only is the plasma dynamic over a given timewindow, the filterscope diagnostic data itself can be very noisey causing ELM detection to be further complicated. Filterscopes are noisy because they are high-frequency diagnostics, which leads to noisy signals when examining naturally unstable plasmas. Figures 3.6 and 3.7 show the reduction in data variance made possible by filtering the ELMs. In order to minimize noise in the filterscope data we chose the filterscope diagnostic closest to the interior strike point, where the plasma touches the wall on the straight part of the D shape. The interior strike point is least susceptible to noise from high frequency plasma fluctuations. Filterscope diagnostics are shown in figure 3.2.

3.2 Preparation

To prepare the data for my analysis, we sorted it into ascending magneto-radial order and selected data within the pedestal region of the plasma, from 85% to 110% of the magneto-radius of the plasma. I then extracted the Thomson Scattering times from the last 20% of each ELM cycle, excluding times before the first and last observed ELMs in the last 20% of the cycles. Since the plasmas are dynamic, even data taken within the same section of the ELM cycle will be affected over time. To limit the effects of drifting plasma parameters over time, I used only the first 5 cleaned time slices from each discharge. For each time slice in each discharge, we further cleaned the data by selecting the temperature and density data from these limited time slices across the pedestal, removing any erroneous values in the data. After cleaning each time slice, we consolidated the cleaned data into a single data sample and normalized the densities to their max values. We then fit a tanh curve to the density data over the pedestal region using the equation

$$y = \frac{h}{2}(tanh(\frac{2}{w}(x0 - x)) + 1) + e \tag{3.1}$$

where h is the height of the pedestal, x0 is the center location of the fit, w is the distance of the fit from the center point to the edge, and e is the offset.

These fits yield on average an adjusted R^2 value above 0.95, indicating that the fit captures most of the variation in the data. To ensure regularity between plasmas, I shifted the radial locations of each shot so that the normalized magneto-radius, Ψ_n, equals 1 where the plasma edge temperature is 100eV. Figures 3.8 and 3.9 show fits for a HighIp plasma with consistent ELM patterns and a closed divertor plasma with inconsistent ELM patterns.

3.3 Analysis and Results

3.3.1 Analytical Method

To investigate the role of fueling on density at the edge, we analyzed relationships between density parameters and fueling using linear regressions. These density parameters were density at the scrape off layer (Ne_{SOL}), density at the top of the pedestal (Ne_{Ped}), the difference in densities across the pedestal (Δ_{Ne}), the normalized difference in densities across the pedestal using the height parameter from the fits (h), and the width of the pedestal using the width parameter from the fits (w).

We quantify the relationships and our confidence in them with coefficient values and p-values for each linear fit. The coefficients describe the estimated relationship between the fueling and the density parameters of interest while the p-values describe the statistical probability that the estimated coefficients are statistically significantly different from 0, i.e. there not being a relationship at all. P-values less than 0.05 indicate statistical significance at the 5% level, while p-values less than 0.01 indicate statistical significance at the 1% level. In general, smaller p-values indicate increased confidence in the regression coefficient, and any coefficient with a p-value in excess of 0.05 will not be considered statistically significant.

3.3.2 Aggregate Results

We first plotted the variables of interest vs fueling with their linear fits to get a feel for the data collectively instead of immediately separating each plasma type for analysis. We observe correlations between scrape off layer density and fueling levels as well as pedestal density and fueling levels, shown in figure 3.10. We observed positive correlations between the density difference across the pedestal for open divertor configuration plasmas, but a negative correlation for closed divertor plasmas, shown in figure 3.11.

We found negative correlations for the height for all plasmas, but we found conflicting relationships for width: negative for high-current open divertor, positive for low current closed divertor, and no correlation for low current open divertor. These are shown in figure 3.12.

3.3.3 In Depth Results

We then examined each correlation individually in order to gain more robust knowledge of the relationships as well as explore differences between plasma types. Using matlab's statistical software package, we examined the coefficients and p-values for each density parameter correlation, separated by plasma type.

Scrape Off Layer

Examining the scrape off layer density vs the fueling broken down by each plasma type reveals the following table. With a P-value of 0.604, we did not find the scrape off layer density of closed divertor plasmas to be statistically significantly correlated to Fueling levels. However, for both open divertor groups we did find statistically significant correlation. We would expect an additional Torr×L/s of fueling to be connected to an increase in density of $5 \times 10^{16}/m^3$ for low current plasmas and $3.6 \times 10^{16}/m^3$ for the high current plasmas. The correlation data is in table 3.1 and in figure 3.13.

Configuration	Coefficient (10^{19})	P-value
Open	0.0050	0.008
Closed	0.0038	0.604
HighIp	0.0036	0.004

Table 3.1: Regression statistics for scrape off layer density vs fueling.

Pedestal Density

Examining the pedestal density vs the fueling broken down by each plasma type reveals the following table. With a P-value of 0.825, we did not find the scrape off layer density of closed divertor plasmas to be statistically significantly correlated to Fueling levels. However, for both open divertor groups we did find statistically significant correlation. We would expect an additional Torr×L/s of fueling to be

connected to an increase in density of $1.6 \times 10^{17}/m^3$ for low current plasmas and $7 \times 10^{16}/m^3$ for the high current plasmas. The correlation data is in table 3.2 and in figure 3.14.

Configuration	Coefficient (10^{19})	P-value
Open	0.026	0.005
Closed	0.001	0.825
HighIp	0.007	0.010

Table 3.2: Regression statistics for pedestal density vs fueling.

Density Difference

Examining the density difference across the pedestal vs the fueling broken down by each plasma type reveals the following table. With a P-value of 0.722, we did not find the scrape off layer density of closed divertor plasmas to be statistically significantly correlated to Fueling levels. However, for both open divertor groups we did find statistically significant correlation. We would expect an additional Torr×L/s of fueling to be connected to an increased difference in density across the pedestal of $1.07 \times 10^{17}/m^3$ for low current plasmas and $3.4 \times 10^{16}/m^3$ for the high current plasmas. The correlation data is in table 3.3 and in figure 3.15.

Configuration	Coefficient (10^{19})	P-value
Open	0.0107	0.031
Closed	-0.0026	0.722
HighIp	0.0034	0.031

Table 3.3: Regression statistics for the change in density across the pedestal vs fueling.

Height

Examining the height parameter of the pedestal fits vs the fueling broken down by each plasma type reveals the following table. With p-values of 0.281 and 0.637

respectively, we did not find the pedestal heights to be statistically significantly correlated to Fueling levels for any low current plasmas. However, for high current plasmas we did find a statistically significant correlation. We would expect an additional Torr×L/s of fueling to be connected to a decreased pedestal height of 0.03% of the maximum fit data point. The correlation data is in table 3.4 and in figure 3.16.

Configuration	Coefficient	P-value
Open	-0.0003	0.281
Closed	-0.0006	0.637
HighIp	-0.0003	0.040

Table 3.4: Regression statistics for the height parameter across the pedestal vs fueling.

Width

Examining the width parameter of the pedestal fits vs the fueling broken down by each plasma type reveals the following table. With p-values of 0.884, 0.767 and 0.106, we did not find the pedestal widths to be statistically significantly correlated to Fueling levels for any grouping of discharges. The correlation data is in table 3.5 and in figure 3.17.

Configuration	Coefficient (10^{-6})	P-value
Open	-2.78	0.884
Closed	121	0.767
HighIp	-36.6	0.106

Table 3.5: Regression statistics for the width parameter across the pedestal vs fueling.

3.3.4 Analysis of Results

To investigate the relative effects of fueling at the scrape off layer compared to the pedestal top, we compared coefficient estimates to the average parameter values. We observe relatively high expected changes in density from additional fueling at the scrape off layer. At the scrape off layer, the expected increase in density from an

additional Torr×L/s of fueling is 0.5% of the average scrape off layer density for the low current plasmas and 0.3% for the high current plasmas. At the pedestal, the expected relative increase in density is 0.26% for low current plasmas and 0.09% for high current plasmas. The relative increases from fueling in scrape off layer density of 0.5% and 0.3% are higher than the relative increases in pedestal density of 0.26% and 0.09%, illustrating more pronounced effects from fueling in the scrape off layer.

Additionally, we also observe higher relative changes in density across the pedestal compared to the relative changes in expected fueling effects across the pedestal. The ratio of the pedestal density to the scrape off layer density is 6.1 and 6.525 for low current and high current plasmas respectively. However, the ratio of expected pedestal density increases to expected scrape off layer density increases is 3.2 and 1.94 for low current and high current plasmas respectively. The increases in expected effects of fueling on density across the pedestal are smaller than the increases in density across the pedestal, further suggesting a relatively strong fueling effects at the scrape off layer.

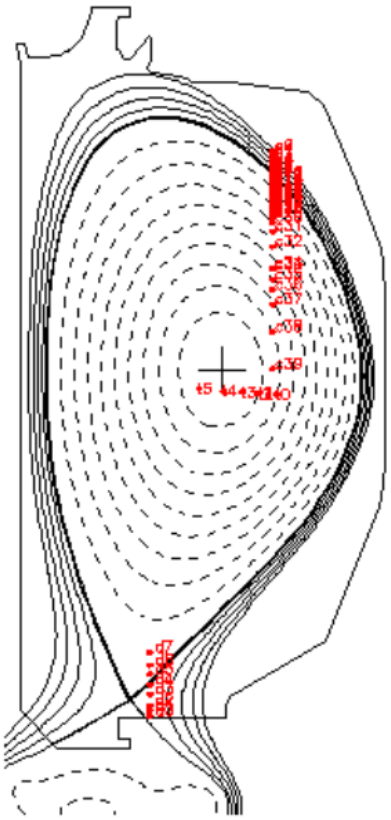

Figure 3.1: Thomson Scattering diagnostic measurement points (red) overlayed onto a plasma cross section. To compare the Thomson Scattering data we need to change coordinate systems to control for magnetic and radial differences in the plasma.

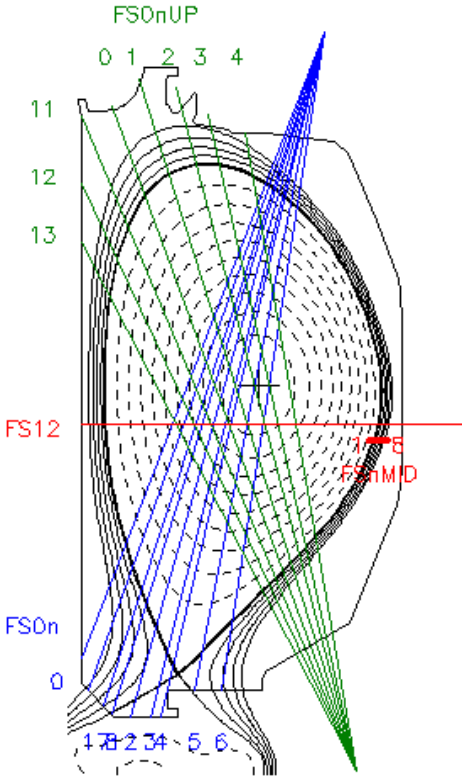

Figure 3.2: Filterscope diagnostic measurement points (blue and green) overlayed onto a plasma cross section. The filterscope diagnostic that experiences the least noise in its signal is the diagnostic closes to the strike point, which in this case is FS01.

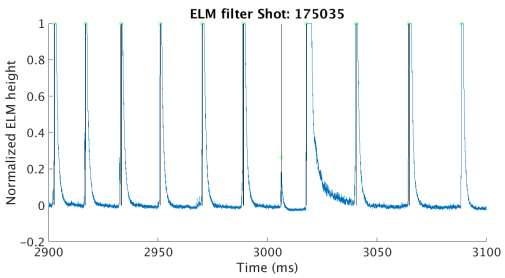

Figure 3.3: ELM cycles over time in a relatively predictable plasma with consistent ELM patterns. Using a critical filter value works well for this data.

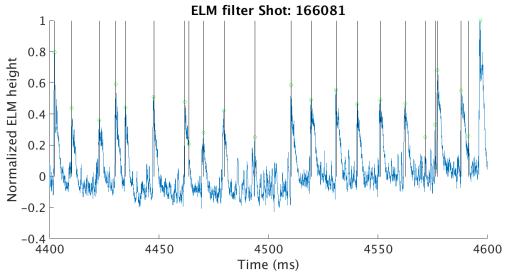

Figure 3.4: ELM cycles over time in a relatively messy plasma with inconsistent ELM patterns. Using a critical filter value ignores the dynamics of the plasma, making it a suboptimal filtering technique.

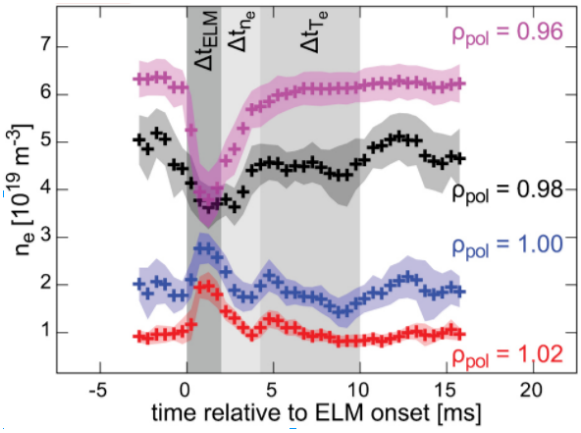

Figure 3.5: Time response of plasma through an ELM cycle. After about 10ms the density values are stable at their equilibrium levels again. This figure shows the density across the pedestal from just inside the edge at $\rho = 0.96$ to just outside at $\rho = 1.02$. We see a drop in density inside that recovers back to normal levels, while we see a peak in density outside that recovers back to normal levels [4].

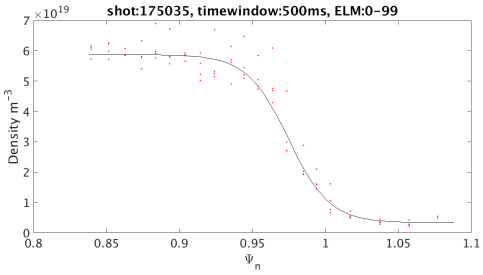

Figure 3.6: Data dispersion and tanh fit for a HighIp plasma without filtering ELM patterns.

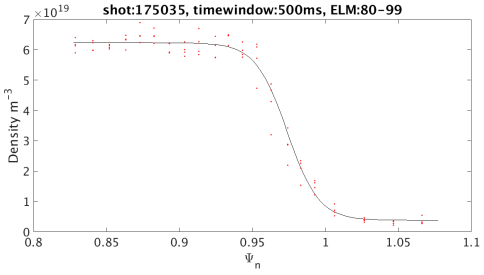

Figure 3.7: Data dispersion and tanh fit for a HighIp plasma with ELM filtering. The spread of the data with filtering is substantially lower than without filtering, making the fits more dependable.

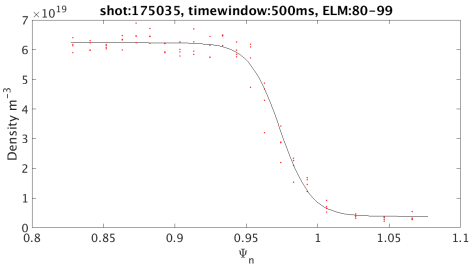

Figure 3.8: Tanh fit for a filtered HighIp plasma with consistent ELMs .

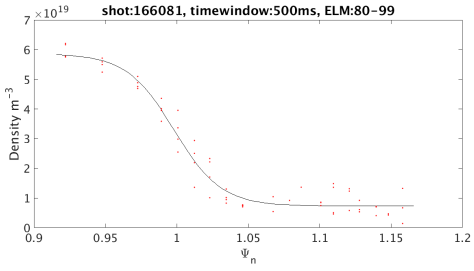

Figure 3.9: Tanh fit for a filtered closed divertor plasma with inconsistent ELMs.

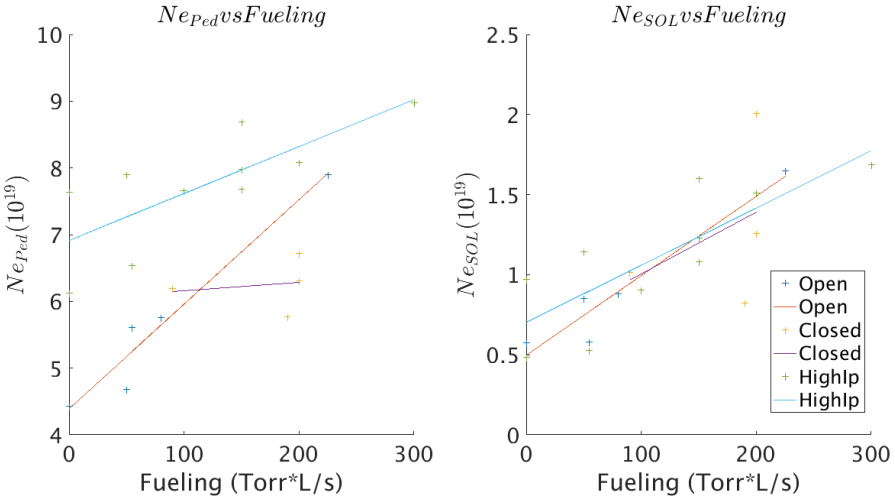

Figure 3.10: Ne_{SOL} and Ne_{Ped} vs fueling for each plasma type Find very similar relationships for the scrape off layer, but more diverse relationships for the pedestal top.

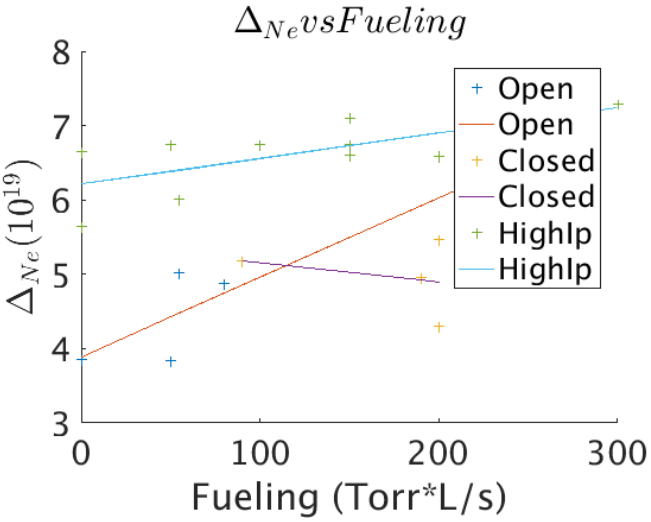

Figure 3.11: The difference in density across the pedestal vs fueling for all plasma types. The difference in density gives insight into how fueling increases density at the pedestal top and scrape off layer at the same time. We see than in terms of scale, the top of the pedestal increases by more than the base.

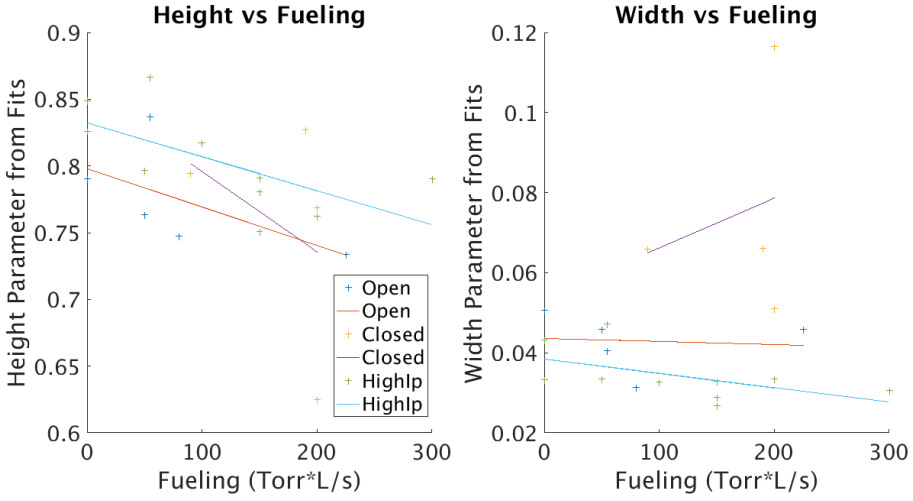

Figure 3.12: The pedestal fit parameters for height and width vs fueling. Pedestal relative height is consistently downward sloping across all plasma types, but pedestal width responses are not as consistent. Both open divertor pedestal widths exhibit negative correlations, but the open divertor plasma width exhibits a postive correlation to fueling.

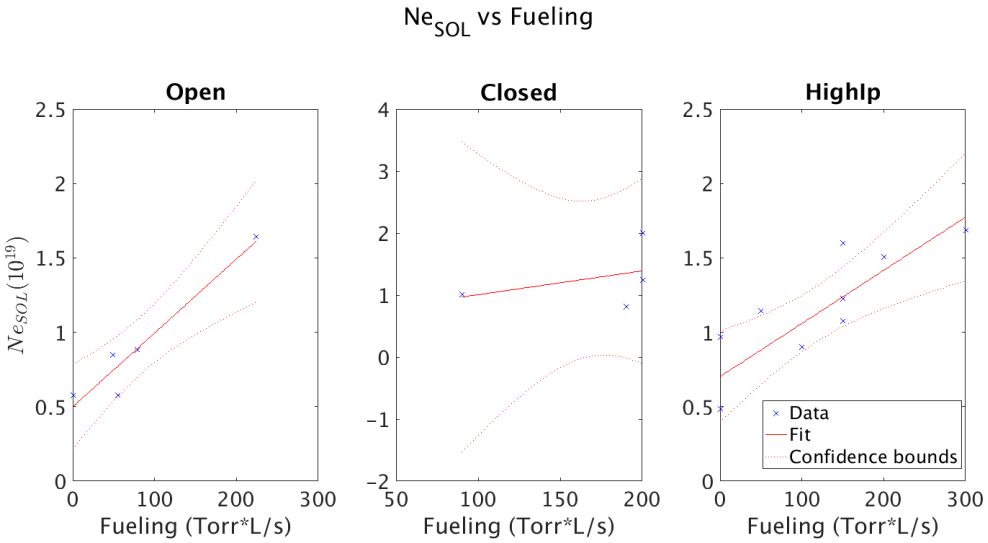

Figure 3.13: Density at the scrape off layer vs fueling separated by plasma type. Only the open divertor plasmas have significant correlations with fueling. The correlations were very similar despite varied plasma conditions.

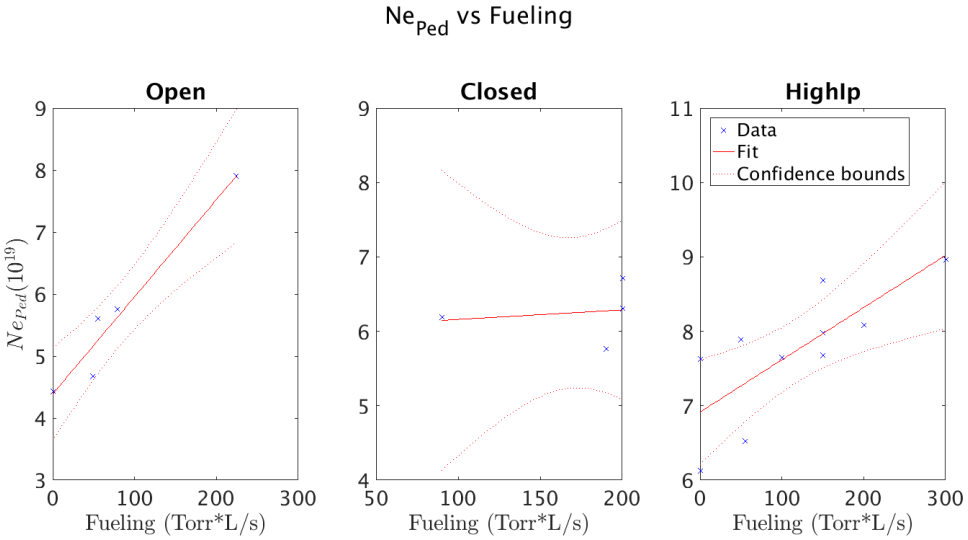

Figure 3.14: Density at the pedestal vs fueling separated by plasma type. Only the open divertor plasmas have significant correlations with fueling. Found more disparate correlations with fueling than the scrape off layer density.

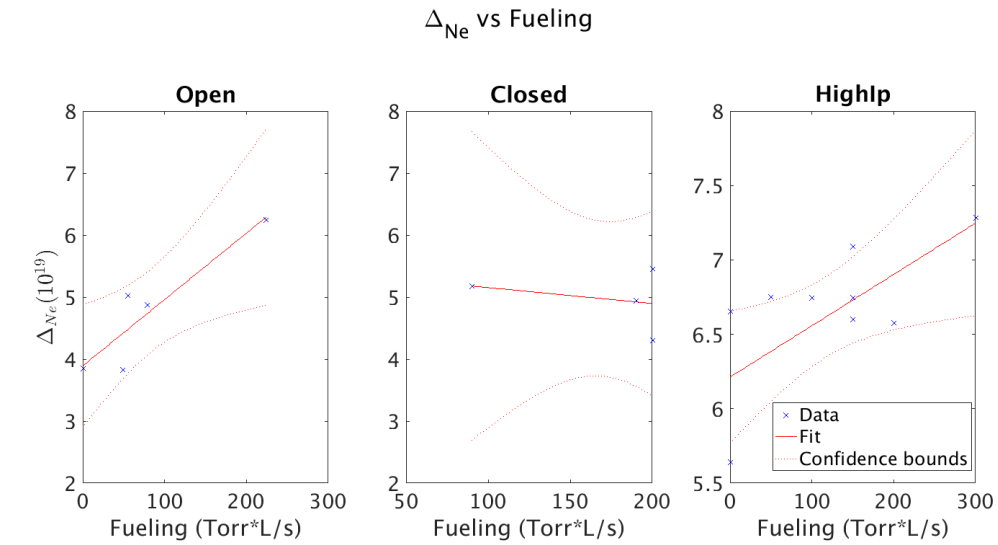

Figure 3.15: Density difference across the pedestal vs fueling separated by plasma type. Only the open divertor plasmas have significant correlations with fueling. The lower density Open plasmas has more significant growth across the pedestal than HighIp plasmas.

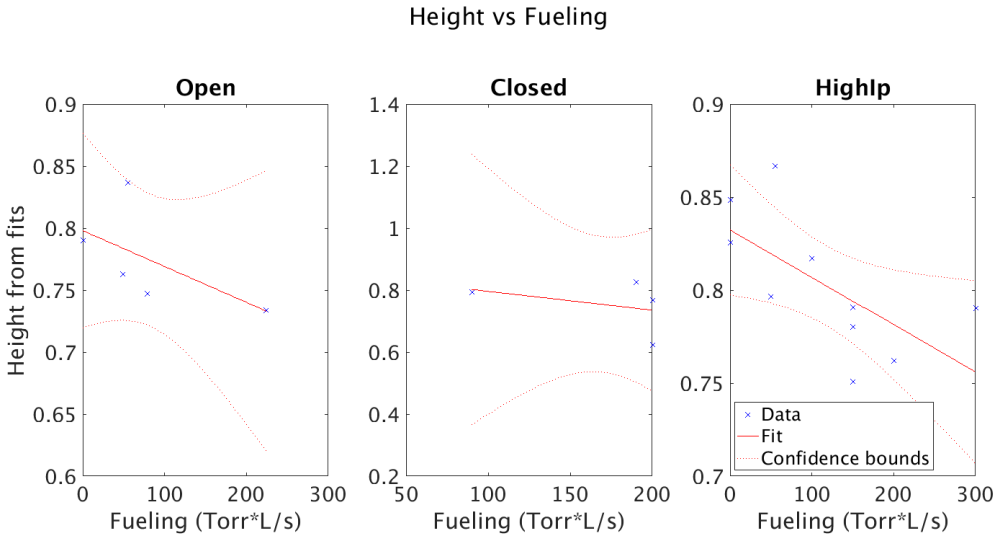

Figure 3.16: Normalized pedestal height parameter vs fueling separated by plasma type. Only the high current plasmas have significant correlations with fueling.

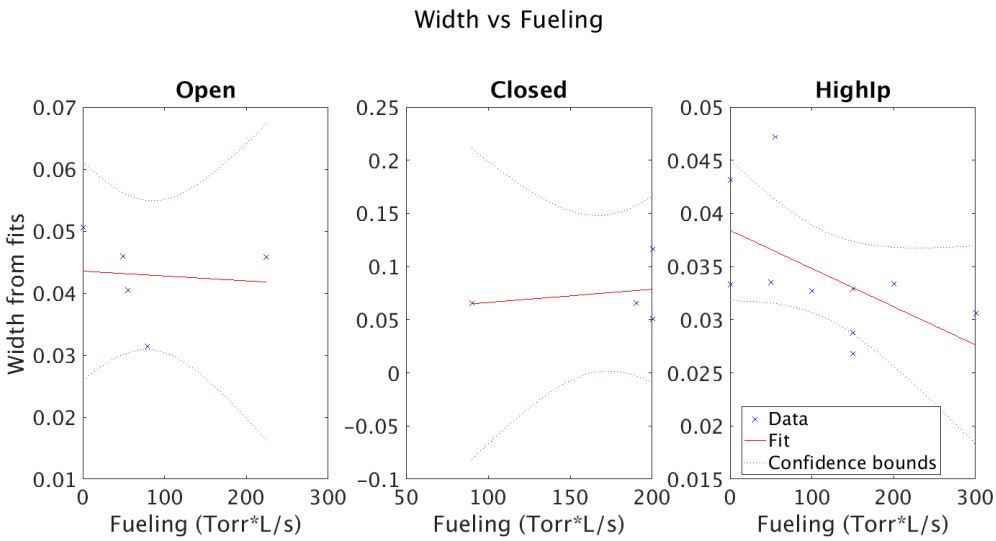

Figure 3.17: Pedestal width parameter vs fueling separated by plasma type. None of the plasma types had significant correlations with fueling.

Chapter 4

Conclusions and Future Plans

4.1 Conclusions

We found strong correlations between pedestal density profiles and fueling for open divertor plasmas that indicate neutral fueling increases density at the edge. We found statistically significant positive correlations between fueling and density at the scrape off layer, density at the top of the pedestal, and density growth across the pedestal. These regressions do not sufficiently demonstrate causation on their own. However, since fueling was the primary independent variable across these plasmas, it is likely that the observed increases in density and density growth were influenced by increased fueling. This is consistent with the theory of neutral fueling: neutral gas that is pumped into the chamber diffuses into the plasma and ionizes, increasing the density of the pedestal region of the plasma.

We observed more pronounced density increases from fueling at the scrape off layer than the pedestal top. When neutral gas diffuses into plasma, it can penetrate only as far as it remains neutral, i.e. until it ionizes. The scrape off layer is at the edge of the plasma, so most of the neutral gas will penetrate to the scrape off layer. However, as the fuel moves further into the pedestal region, the plasma becomes more dense and ionization occurs more rapidly. The increased ionization rate in conjunction with

longer travel distance suggests that fueling will not affect the pedestal top as much because less fuel will remain neutral by the time it reaches the pedestal top. Even as neutral fueling does not have large direct effects on the plasma beyond the pedestal, the effects of neutral fueling on the pedestal region cascade to other parts of the plasma through other interrelated plasma effects.

We found that the width of the pedestal is not statistically significantly related to fueling for either the low or high current plasmas, indicating that fueling does not have consistent effects on the width of the pedestal. This implies that neutral ionization rates do not significantly increase with fueling. If fueling increased ionization rates, neutrals would travel less distance and the pedestal width would contract. We would expect this effect to be more present in plasmas with pronounced pedestals wherein fueling is even more localized to the scrape off layer. Even though the relationship is not statistically significant, a negative correlation between width and fueling is observed in the high current plasmas which have the smallest widths and largest density increases across the pedestal. This relationship is unobserved in the lower density plasmas. With even higher densities and thinner pedestals we might expect to see a statistically significant relationship between fueling and pedestal width.

We found differences between closed divertor and open divertor plasma responses to fueling. For the closed divertor, no correlations between density and fueling were statistically significant, even when the relationships were very statistically significant for open divertor plasmas. This could indicate that divertor geometry is an important factor to consider when evaluating fueling effects on the pedestal density. Closed divertor plasmas are more strongly connected to the cryo-pump than open divertor plasmas. This allows for more efficient removal of neutrals from plasmas, reducing the effectiveness of neutral gas fueling on closed divertor plasmas. Even with this in mind, the pronounced difference in fueling effects on density between the divertor

geometries suggests that divertor geometry should be investigated more for how it might affect other neutral related processes. The data set for the closed divertor was relatively small and had the noisiest filterscope data. As a result, more analysis is needed to understand how fueling effects differ between closed divertor plasmas and open divertor plasmas.

4.2 Future Study

The density data points in the plasmas of this analysis varied at the same magneto-radial location due to plasma instabilities. To address this, we filtered the data with respect to ELM cycles, but even with the filtering there was substantial variation in the data. This variation comes partially from ELM effects which the filtering was unable to entirely control for, and improving the ELM filtering function would help reduce this variation. Reducing the data spread by improving the ELM filtering function would improve the reliability of the density profile fits which were used to investigate the role of fueling on density at the edge.

This analysis investigated the relationship between fueling and the pedestal density profile by inspecting correlations between increased neutral gas fueling and various components of the density profile. While we found significant relationships between fueling and the density profile, we did not directly control for effects of other variations in the plasma as fueling increases. In the future, it would be beneficial to investigate the effects of fueling on other parameters that might also impact the density profile.

This analysis found significant relationships between fueling and the pedestal density profile for open divertor plasmas. However, there were not significant relationships for closed divertor plasmas. Closed divertor plasmas respond differently to fueling because of the reduced ventilation in the chamber, but questions remain about

what other effects divertor geometry has on plasmas.

Because this analysis exclusively used data from DIII-D, its results would be strengthened through corroboration from other fusion research facilities. If we performed a similar analysis on suitable plasmas from different tokamaks around the world, we would be able to know more definitively how fueling affects pedestal density profiles, giving more dependable insight into transport theory at the edge.

Bibliography

[1] No Author. European joint undertaking for iter and the development of fusion energy: What is fusion?, 2015.

[2] R.J. Groebner, C.S. Chang, J.W. Hughes, R. Maingi, P.B. Snyder, X.Q. Xu, J.A. Boedo, D.P. Boyle, J.D. Callen, J.M. Canik, I. Cziegler, E.M. Davis, A. Diallo, P.H. Diamond, J.D. Elder, D.P. Eldon, D.R. Ernst, D.P. Fulton, M. Landreman, A.W. Leonard, J.D. Lore, T.H. Osborne, A.Y. Pankin, S.E. Parker, T.L. Rhodes, S.P. Smith, A.C. Sontag, W.M. Stacey, J. Walk, W. Wan, E.H.-J. Wang, J.G. Watkins, A.E. White, D.G. Whyte, Z. Yan, E.A. Belli, B.D. Bray, J. Candy, R.M. Churchill, T.M. Deterly, E.J. Doyle, M.E. Fenstermacher, N.M. Ferraro, A.E. Hubbard, I. Joseph, J.E. Kinsey, B. LaBombard, C.J. Lasnier, Z. Lin, B.L. Lipschultz, C. Liu, Y. Ma, G.R. McKee, D.M. Ponce, J.C. Rost, L. Schmitz, G.M. Staebler, L.E. Sugiyama, J.L. Terry, M.V. Umansky, R.E. Waltz, S.M. Wolfe, L. Zeng, and S.J. Zweben. Improved understanding of physics processes in pedestal structure, leading to improved predictive capability for iter. *Nuclear Fusion*, 53(9):093024, 2013.

[3] Matthias Hirsch. Tokamak schema from the wikimedia commons.

[4] F.M. Laggner, E. Wolfrum, M. Cavedon, M.G. Dunne, G. Birkenmeier, R. Fischer, M. Willensdorfer, F. Aumayr, The EUROfusion MST1 Team, and The ASDEX Upgrade Team. Plasma shaping and its impact on the pedestal of asdex

upgrade: edge stability and inter-elm dynamics at varied triangularity. *Nuclear Fusion*, 58(4):046008, 2018.